

RESEARCH

Open Access



Effect of glycemic status on myocardial deformation and microvascular function in uncomplicated pediatric type 1 diabetes mellitus: cardiac magnetic resonance imaging

Lu Zhang^{1,2†}, Shan Huang^{1,2†}, Xueming Li³, Zhi Yang⁴, Pengfei Ye^{1,2}, Ran Sun¹, Huayan Xu^{1,2}, Rong Xu^{1,2}, Meng Zhang¹, Ying Liu⁵, Chuanjie Yuan⁵, Jin Wu^{5*} and Yingkun Guo^{1,2*}

Abstract

Background Cardiovascular disease remains the leading cause of morbidity and mortality among individuals with type 1 diabetes mellitus (T1DM). Individuals with hyperglycemia are at great risk of cardiovascular complications. This study investigated the impact of glycemic control on left ventricular (LV) microvascular perfusion and myocardial deformation in uncomplicated pediatric T1DM using cardiac magnetic resonance (CMR) imaging.

Methods A total of 100 uncomplicated pediatric patients with T1DM and 35 controls were enrolled and underwent 3.0 T CMR examinations. Patients were divided into two groups according to HbA1c levels of 7.0% (HbA1c < 7.0%, n = 25; HbA1c ≥ 7.0%, n = 75). Subclinical systolic and diastolic function were evaluated using peak strain and strain rate based on myocardial deformation analysis. Myocardial perfusion upslope and maximum signal intensity (MaxSI) were assessed via first-pass perfusion imaging at rest. Multivariable linear regression analyses identified the independent factors of reduced myocardial perfusion and deformation in T1DM patients.

Results Among the three groups, longitudinal peak diastolic strain rate (PDSR) deteriorated gradually from controls through patients with HbA1c < 7.0% to patients with HbA1c ≥ 7.0% (all $p < 0.05$). Upslope in patients with HbA1c ≥ 7.0% was decreased compared to patients with HbA1c < 7.0% ($p = 0.007$) and controls ($p < 0.001$). Compared to controls, both MaxSI and circumferential PDSR were reduced in patients with HbA1c ≥ 7.0% ($p = 0.025$ and 0.016 , respectively), but not in patients with HbA1c < 7.0% ($p = 0.566$ and 0.379 , respectively). In multivariable analysis, elevated HbA1c level was independently associated with reduced upslope ($\beta = -2.53$, $p < 0.001$) and longitudinal PDSR ($\beta = -0.02$, $p = 0.007$). When the perfusion indices were included in the multivariable analysis for diastolic dysfunction, upslope ($\beta = 0.10$, $p = 0.016$) and MaxSI ($\beta = -0.02$, $p = 0.006$) were associated with reduced longitudinal PDSR.

[†]Lu Zhang and Shan Huang are co-first authors.

*Correspondence:

Jin Wu
wangdo620@163.com
Yingkun Guo
gykpanda@163.com

Full list of author information is available at the end of the article



© The Author(s) 2025. **Open Access** This article is licensed under a Creative Commons Attribution-NonCommercial-NoDerivatives 4.0 International License, which permits any non-commercial use, sharing, distribution and reproduction in any medium or format, as long as you give appropriate credit to the original author(s) and the source, provide a link to the Creative Commons licence, and indicate if you modified the licensed material. You do not have permission under this licence to share adapted material derived from this article or parts of it. The images or other third party material in this article are included in the article's Creative Commons licence, unless indicated otherwise in a credit line to the material. If material is not included in the article's Creative Commons licence and your intended use is not permitted by statutory regulation or exceeds the permitted use, you will need to obtain permission directly from the copyright holder. To view a copy of this licence, visit <http://creativecommons.org/licenses/by-nc-nd/4.0/>.

Conclusion Pediatric T1DM with higher HbA1c showed worse myocardial perfusion and subclinical diastolic dysfunction. Microvascular dysfunction was associated independently with cardiac dysfunction.

Trial registration: retrospectively registered ChiCTR2100043799.

Keywords Type 1 diabetes mellitus, Myocardial strain, Myocardial perfusion, Cardiac magnetic resonance, Glycemic control

Introduction

Type 1 diabetes mellitus (T1DM) is the most common type of childhood diabetes, accounting for approximately 90% of all pediatric diabetes cases [1]. Cardiovascular diseases (CVD) including epicardial coronary artery disease and heart failure remain the leading cause of morbidity and mortality among individuals with T1DM [2, 3]. Individuals diagnosed with T1DM before age 10 face a sevenfold higher CVD mortality risk compared to those non-diabetic peers [4], suggesting that myocardial changes may begin early in childhood-onset T1DM. Early detection of subclinical myocardial injury biomarkers in these patients is crucial for preventing and managing CVD [5]. Studies reporting myocardial microcirculation and subclinical dysfunction in pediatric T1DM patients remain scarce.

Myocardial deformation analysis enables detection of subclinical cardiac dysfunction before left ventricular (LV) ejection fraction (EF) declines, offering insights into early-stage diabetic cardiomyopathy. Additionally, first-pass myocardial perfusion CMR could monitor myocardial microvascular dysfunction non-invasively. Cardiac magnetic resonance (CMR) imaging serves as a sensitive and non-invasive method for detecting myocardial alterations, as recommended for young individuals with T1DM [6].

A large prospective study demonstrated that a 1% increase in HbA1c level was associated with a 30% higher risk of heart failure independently of other CVD risk factors [7]. Poor glycemic control increases microvascular complications in the T1DM population in a 30-year follow-up study [8]. Chronic hyperglycemia is the most critical modifiable factor for CVD in diabetes. However, the relationship between hyperglycemia and diabetic myocardial injury in pediatric T1DM requires further investigation. Therefore, we used CMR to evaluate the effect of glycemic status on LV myocardial deformation in uncomplicated pediatric T1DM. We further incorporated myocardial perfusion imaging to unmask subtle changes in myocardial microvascular function that might compromise cardiac performance.

Materials and methods

This study was approved by the Biomedical Research Ethics Committee of our hospital and conducted in accordance with the Declaration of Helsinki. Written informed

consent was obtained from all the participants' legal guardian prior to inclusion in the study.

Study population

From June 2019 to May 2024, pediatric T1DM patients (<18 years) were enrolled at our institution. The inclusion criterion was the diagnosis of T1DM based on the guidelines by the American Diabetes Association guidelines. The exclusion criteria were as follows: (1) individuals with established cardiovascular disease (e.g., myocarditis and congenital cardiovascular); (2) those with contraindications to CMR imaging (claustrophobia, implanted pacemakers); (3) individuals with diabetic macrovascular and microvascular complications (retinopathy, nephropathy, peripheral neuropathy, autonomic neuropathy) as assessed by the endocrinologists; (4) incomplete imaging results or poor CMR image quality that affecting LV measurements; (5) missing biochemical data.

Using G*Power 3.1.9.7 (Heinrich-Heine-Universität Düsseldorf, Germany), we performed a one-way ANOVA based on preliminary longitudinal peak diastolic strain rate data [9]. With $\alpha=0.05$ (95% confidence) and power=0.80, the analysis required 22 participants per group. Accounting for a 10% dropout rate, we included 75 participants (25 per group). Of 110 screened T1DM patients, 100 met eligibility criteria (see Fig. 1 for flowchart).

Clinical and biochemical assessments

Before CMR examinations, we recorded blood pressure [systolic blood pressure (SBP) and diastolic blood pressure (DBP)] and anthropometric measurements [body weight, height, hip, waist circumference, body mass index (BMI), and body surface area (BSA)] and collected fasting blood samples for analysis. Laboratory measurements included glucose metabolism [Fasting plasma glucose (FPG) and glycated hemoglobin (HbA1c)], lipid profile [Total cholesterol (TC), triglycerides (TG), high-density lipoprotein (HDL), low-density lipoprotein (LDL), and apolipoprotein A1 (ApoA1)], renal function (Urea nitrogen, creatinine, uric acid, and cystatin C).

Patient stratification

Per the 2024 American Diabetes Association and 2020 Chinese guidelines [10, 11], which both recommend a glycemic target of <7.0% HbA1c for pediatric T1DM,

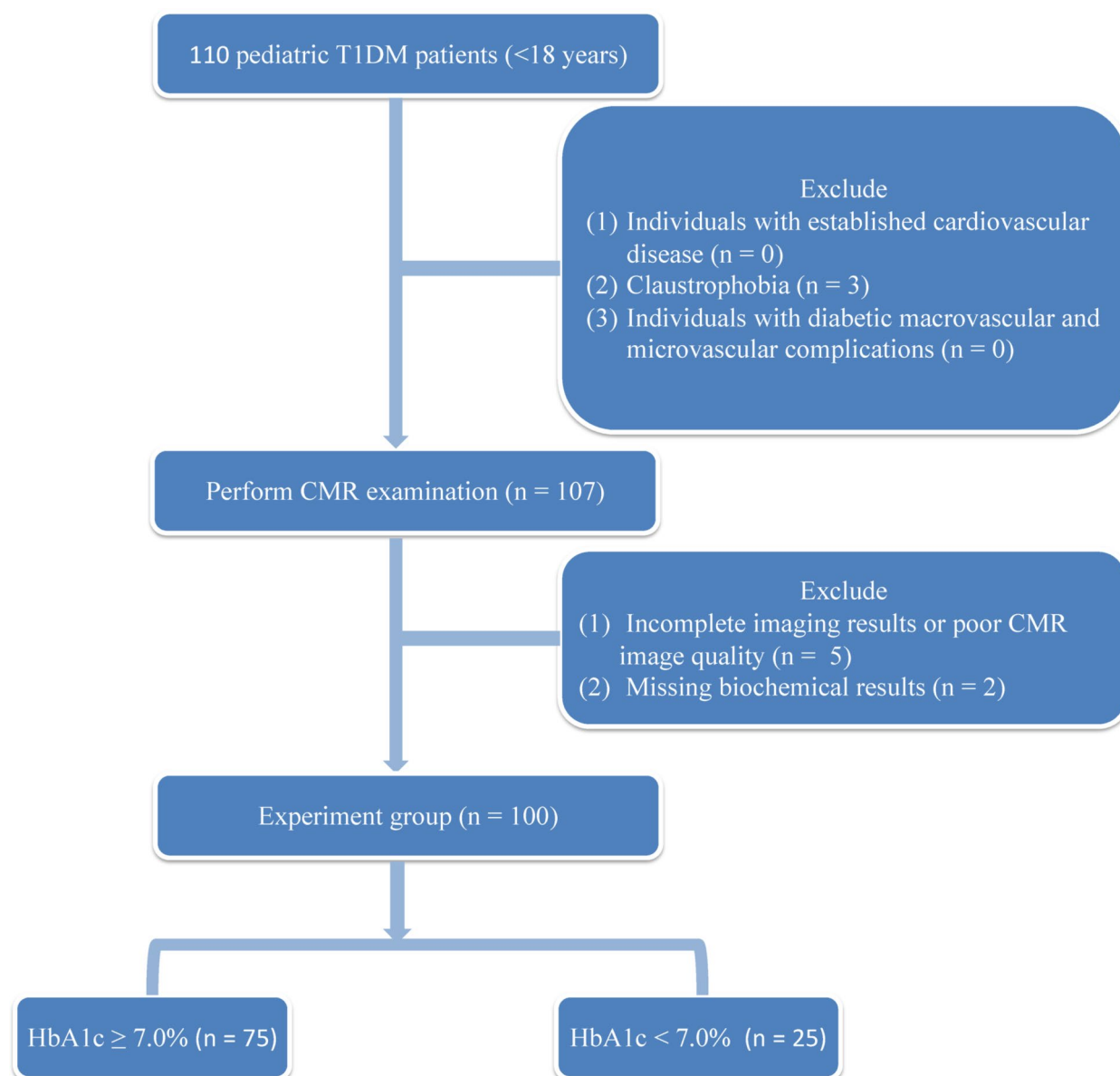


Fig. 1 Flowchart of the cohort study. T1DM, type 1 diabetes mellitus; CMR, cardiac magnetic resonance

we stratified patients into two groups: HbA1c < 7.0% and HbA1c ≥ 7.0%. Age- and sex-matched controls were also enrolled and underwent the same CMR protocol.

CMR protocols

All CMR scans were performed using a 3.0T scanner (MAGNETOM Skyra, Siemens Healthcare, Erlangen, Germany) equipped with an 18-channel receive coil. ECG-gated cine images were acquired using a balanced steady-state free-precession sequence during breath-holds (5–8 s), covering the LV with 8–12 contiguous short-axis slices from mitral valve to apex (thickness 6 mm, TR/TE 3.42/1.48 ms, matrix 126 × 224, FOV 300 × 320 mm²). First-pass perfusion imaging was

obtained at rest following intravenous administration of gadobutrol (Gadovist, Bayer Healthcare, 0.1 mL/kg at 1–2 mL/s) using an inversion recovery echo-planar sequence in three short-axis (thickness 6 mm, TR/TE 2.20/1.10 ms, flip angle 10°, matrix 98 × 192, FOV 270 × 360 mm²). LGE images were acquired 5–10 min post-contrast using phase-sensitive inversion recovery (thickness 6 mm, TR/TE 2.55/1.10 ms, flip angle 55°, matrix 128 × 192, FOV 340 × 360 mm²).

Postprocessing of CMR images

All CMR parameters were measured using commercially available software (CVI⁴²; Circle Cardiovascular Imaging, Inc., Calgary, Canada) by two experienced CMR

radiologists. LV endocardial and epicardial borders were initially delineated automatically followed by manual adjustment at end-diastolic and end-systolic phases. LV end-diastolic volume (EDV), end-systolic volume (ESV), and mass (LVM) were measured and indexed to body surface area (BSA) as LVEDVi, LVESVi, and LVMi. Myocardial strain analysis employed feature-tracking technology to derive global peak strain, peak diastolic (PDSR) and systolic (PSSR) strain rates in radial, circumferential, and longitudinal dimensions. Perfusion parameters were measured through time-intensity curve analysis of basal, mid, and apical slices, generating upslope, maximum signal intensity (MaxSI), time-to-MaxSI (TTM), and perfusion index (myocardial-to-blood pool upslope ratio).

Reproducibility of LV strain and first-pass myocardial perfusion parameters

The reproducibility of CMR parameters was assessed by re-measuring LV global strain and myocardial perfusion parameters in 40 randomly selected cases. Intra-observer variability was determined by reanalyzed after 1 month by the original investigator (L.Z. with 6 years of experience). Interobserver variability was determined by a second blinded investigator (S.H. with 6 years of experience) evaluating the same cohort independently.

Statistical analysis

Statistical analyses were performed using SPSS version 23.0 (IBM, Armonk, New York, USA), GraphPad Prism 9 (GraphPad Software, San Diego, CA, USA), and R studio (version 4.1.2, <http://www.r-project.org/>). Normally distributed continuous variables are presented as mean \pm standard deviation (SD), while non-normally distributed variables are expressed as median with interquartile range. Non-normally distributed data were log-transformed prior to analysis. Group comparisons were conducted using one-way ANOVA with Bonferroni correction for normally distributed variables and Kruskal-Wallis test for non-normally distributed variables. Categorical variables are presented as percentages and analyzed using Chi-square tests. Associations between clinical variables and CMR parameters were also examined using Pearson's or Spearman's coefficients. Multivariable linear regression analysis was employed to identify independent predictors of myocardial perfusion and strain parameters (positive values) in T1DM. Potential predictors without multicollinearity were selected based on a p -value < 0.1 in the univariable linear regression analysis or clinical relevance. If the variance inflation factor (VIF) ≥ 5 and tolerance ($1/\text{VIF}$) < 0.1 , multicollinearity exists. The intraclass correlation coefficient (ICC) was used to assess the inter- and intra-observer reproducibility. An ICC above 0.8 was considered to be excellent. ICC was interpreted with: $< 0.50 =$

poor; $0.50 \leq \text{ICC} < 0.75 =$ moderate; $0.75 \leq \text{ICC} < 0.90 =$ good; $> 0.90 =$ excellent [95% confidence interval (CI) calculated from 2-way random-effects models [12]. All statistical tests were two-sided, with $p < 0.05$ considered statistically significant.

Results

Baseline characteristics of the participants

The T1DM cohort included 100 T1DM stratified by glycemic control [$\text{HbA1c} < 7.0\%$ ($n=25$) vs. $\text{HbA1c} \geq 7.0\%$ ($n=75$)] and 35 age- and sex-matched controls. The demographic and clinical characteristics of the enrolled individuals are presented in Table 1. Age, BMI, waist-to-hip ratio, BSA, and SBP were comparable among the three groups (all $p > 0.05$). Median diabetes duration did not differ significantly between T1DM subgroups ($p=0.267$). FBG, TG, HDL, and LDL levels were significantly higher in patients with $\text{HbA1c} \geq 7.0\%$ compared to patients with $\text{HbA1c} < 7.0\%$ (all $p > 0.05$).

Comparisons of CMR-derived LV geometry, deformation, and perfusion parameters

Comparisons of CMR parameters among three groups are summarized in Table 2. No significant differences were observed in LVEDVi, LVESVi, LVEF, LVMi, or LVRI among the groups (all $p > 0.05$). Regarding the strain parameters (Fig. 2 A-C), LV radial and longitudinal peak strain were significantly higher in both patient groups compared to controls, without significant differences between patient subgroups (radial, $36.8 \pm 8.4\%$ vs. $45.2 \pm 4.6\%$ vs. $43.9 \pm 11.9\%$, $p=0.009$; longitudinal, $-13.4 \pm 2.8\%$ vs. $-15.1 \pm 3.7\%$ vs. $-15.1 \pm 2.9\%$, $p=0.002$). Conversely, LV longitudinal PDSR was reduced progressively from controls through patients with $\text{HbA1c} < 7.0\%$ to patients with $\text{HbA1c} \geq 7.0\%$ (1.5 ± 0.5 1/s vs. 1.2 ± 0.2 1/s vs. 1.0 ± 0.2 1/s, $p < 0.001$). Additionally, compared to controls, LV circumferential PDSR was reduced in patients with $\text{HbA1c} \geq 7.0\%$ (1.3 ± 0.3 1/s vs. 1.5 ± 0.4 1/s, $p=0.016$) but preserved in patients with $\text{HbA1c} < 7.0\%$ (1.4 ± 0.4 1/s vs. 1.5 ± 0.4 1/s, $p=0.379$). No significant differences were observed in circumferential peak strain, PSSR from three directions, or radial PDSR (all $p > 0.05$).

First-pass perfusion analysis (Fig. 2D) showed graded microvascular impairment with worsening glycemic control. Patients with $\text{HbA1c} \geq 7.0\%$ showed significantly reduced perfusion upslope compared to patients with $\text{HbA1c} < 7.0\%$ ($p=0.007$) and controls ($p < 0.001$), along with decreased MaxSI compared to controls ($p=0.025$). MaxSI and upslope in patients with $\text{HbA1c} < 7.0\%$ remained comparable to controls (MaxSI, $p=0.566$; upslope, $p=1.000$, respectively). Representative CMR images illustrating these findings were presented in Fig. 3.

Table 1 Baseline characteristics of the included participants

	Controls (n = 35)	Type 1 diabetes mellitus		p
		HbA1c < 7.0% (n = 25)	HbA1c ≥ 7.0% (n = 75)	
Age, years	10.4 ± 2.6	11.2 ± 3.3	13.1 ± 3.1	0.133
Male, n (%)	20 (55.6)	11 (44.0)	13 (44.8)	0.342
Height, cm	144.2 ± 15.9	147.4 ± 16.5	154.3 ± 14.1	0.114
Weight, kg	37.8 ± 13.3	40.4 ± 15.3	44.1 ± 14.0	0.323
BSA, m ²	1.2 ± 0.3	1.3 ± 0.3	1.4 ± 0.3	0.339
BMI, kg/m ²	17.0 ± 4.1	17.8 ± 3.2	18.0 ± 3.5	0.864
SBP, mmHg	106.3 ± 11.1	101.6 ± 10.3	106.0 ± 14.1	0.190
DBP, mmHg	68.4 ± 8.3	56.9 ± 12.8*	67.0 ± 10.0 ^{&}	0.008
Waist-to-hip ratio	–	0.8 ± 0.1	0.8 ± 0.1	0.370
Diabetes duration, years	–	3.6 (2.0, 5.4)	3.0 (3.0, 5.5)	0.267
Age at diagnosis, years	–	7.2 ± 2.8	8.1 ± 3.4	0.137
FBG, mmol/L	–	5.6 (4.5, 11.4)	8.3 (5.0, 11.4) ^{&}	0.010
TC, mmol/L	–	4.0 ± 0.6	4.5 ± 1.1	0.212
TG, mmol/L	–	0.6 ± 0.1	0.9 (0.6, 1.2) ^{&}	< 0.001
HDL, mmol/L	–	1.8 ± 0.4	1.5 ± 0.4 ^{&}	0.012
LDL, mmol/L	–	2.0 ± 0.6	2.5 (1.9, 2.9) ^{&}	0.009
ApoA1, g/L	–	1.6 ± 0.2	1.5 ± 0.3	0.090
Urea Nitrogen, mmol/L	–	5.4 (4.4, 6.1)	5.1 (4.1, 5.8)	0.109
Creatinine, μmol/L	–	39.0 (33.5, 49.0)	38.0 (34.0, 38.0)	0.608
Uric Acid, μmol/L	–	276.0 (213.5, 315)	282.0 (221.0, 328.8)	0.470
Cystatin C, mg/L	–	0.8 ± 0.1	0.8 ± 0.1	0.664

BSA body surface area, BMI body mass index, SBP systolic blood pressure, DBP diastolic blood pressure, FBG fast blood glycemia, TC total cholesterol, TG triglycerides, HDL high-density lipoprotein, LDL low-density lipoprotein. *p < 0.05 compared to controls, [&]p < 0.05 compared to patients with HbA1c < 7.0%

Table 2 CMR characteristics compared among type 1 diabetics and controls

	Controls	T1DM		p
		HbA1c < 7.0%	HbA1c ≥ 7.0%	
Left ventricular geometry				
LVEDVi, ml/m ²	74.0 ± 8.1	80.9 ± 10.4	73.0 ± 10.5	0.822
LVESVi, ml/m ²	28.2 ± 3.4	31.5 ± 6.1	29.0 ± 5.2	0.841
LVEF, %	61.6 ± 4.4	61.5 ± 3.1	61.0 ± 3.9	0.335
LVMi, g/m ²	37.9 ± 5.8	44.9 ± 7.9	38.9 ± 9.4	0.644
LVRI	0.5 ± 0.1	0.5 ± 0.1	0.5 ± 0.1	0.343
Myocardial strain				
Radial peak strain, %	36.8 ± 8.4	45.2 ± 4.6*	43.9 ± 11.9*	0.009
Circumferential peak strain, %	–21.6 ± 3.1	–23.2 ± 1.9	–21.6 ± 2.5	0.521
Longitudinal peak strain, %	–13.4 ± 2.8	–15.1 ± 3.7*	–15.1 ± 2.9*	0.002
Radial PSSR, 1/s	3.4 ± 0.9	2.8 ± 0.8	2.9 ± 0.9	0.122
Circumferential PSSR, 1/s	–1.5 ± 0.3	–1.3 ± 0.2	–1.3 ± 0.3	0.077
Longitudinal PSSR, 1/s	–1.3 ± 0.6	–1.0 ± 0.3	–1.0 ± 0.3	0.181
Radial PDSR, 1/s	–3.4 ± 0.4	–3.5 ± 0.9	–3.2 ± 1.2	0.092
Circumferential PDSR, 1/s	1.5 ± 0.4	1.4 ± 0.4	1.3 ± 0.3*	0.021
Longitudinal PDSR, 1/s	1.5 ± 0.5	1.2 ± 0.2*	1.0 ± 0.2* ^{&}	< 0.001
Myocardial perfusion function				
Upslope, %	4.2 ± 1.4	4.3 ± 1.1	3.1 ± 0.8* ^{&}	< 0.001
TTM, s	30.3 ± 8.4	26.5 ± 8.2	33.7 ± 10.1	0.242
Max SI	39.1 ± 10.9	37.1 ± 8.9	32.7 ± 8.9*	0.029
Perfusion index	0.1 ± 0.02	0.1 ± 0.01	0.1 ± 0.01	0.430

HbA1c hemoglobin A1c, LVEDVi indexed left ventricular end-diastolic volume, LVESVi indexed left ventricular end-systolic volume, LVEF left ventricular ejection fraction, LVRI left ventricular remodeling index, LVMi indexed left ventricular mass, PSSR peak systolic strain rate, PDSR peak diastolic strain rate, TTM time to maximal signal intensity, Max SI maximal signal intensity. *p < 0.05 compared to controls, [&]p < 0.05 compared to patients with HbA1c < 7.0%

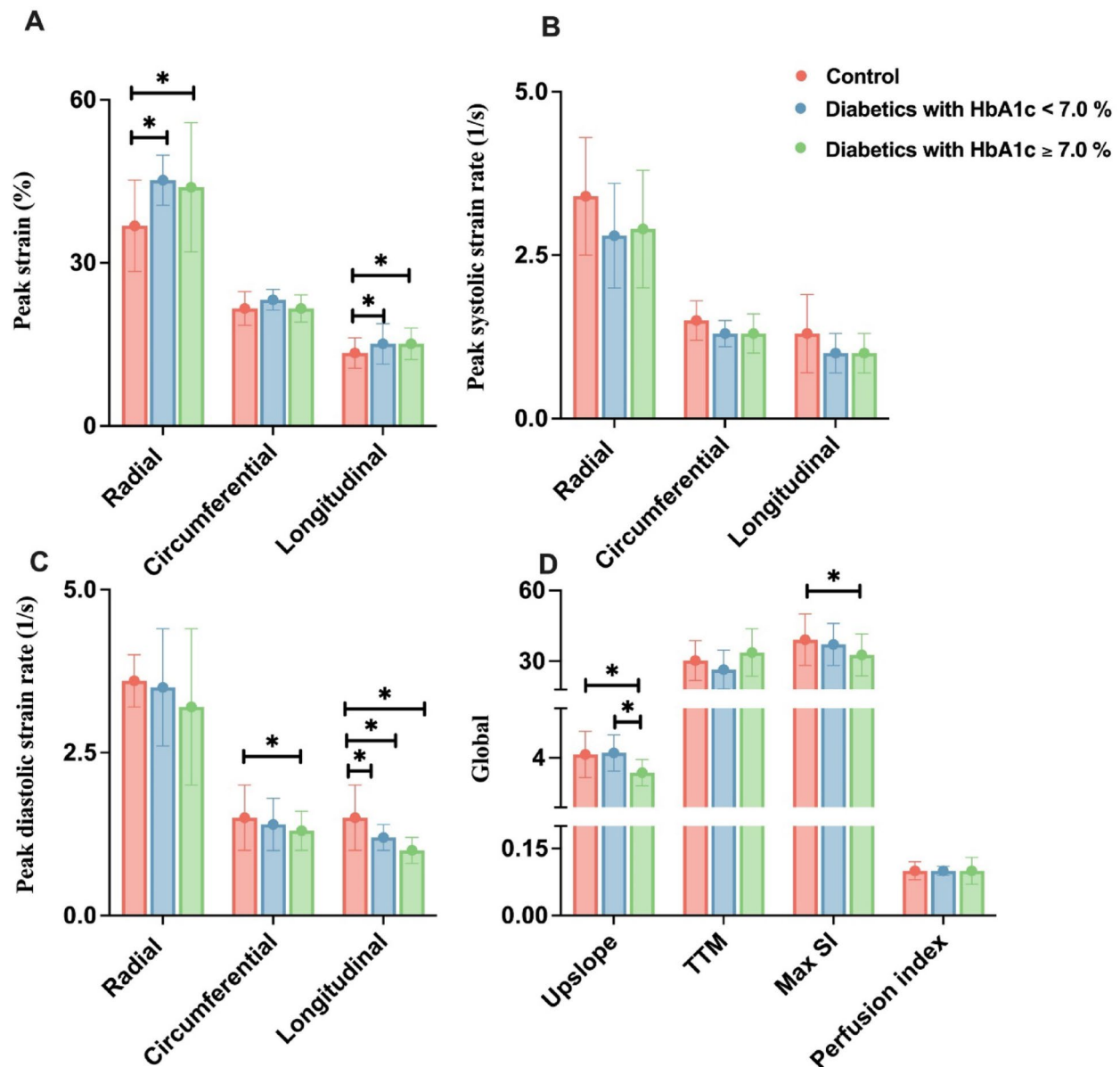


Fig. 2 Comparisons of myocardial strain (the absolute values) and perfusion parameters among type 1 diabetics and controls. Abbreviations: TTM, time to maximal signal intensity; Max SI, maximal signal intensity. * $p < 0.05$.

Univariable and multivariable regression analyses of reduced myocardial perfusion upslope and longitudinal PDSR

Spearman correlation analysis demonstrated a significant inverse correlation between HbA1c levels and myocardial perfusion upslope ($r = -0.482$, $p < 0.001$). Multivariable analyses showed that BMI ($\beta = -0.11$, $p = 0.005$), HbA1c level ($\beta = -2.53$, $p < 0.001$), and LDL ($\beta = 0.40$, $p = 0.021$) were independently associated with upslope after adjustment for other variables (Table 3).

Spearman correlation analysis demonstrated that myocardial perfusion upslope was negatively correlated with longitudinal PDSR ($r = -0.246$, $p = 0.023$). Multivariable

analyses showed that BMI ($\beta = -0.02$, $p = 0.030$), HbA1c level ($\beta = -0.02$, $p = 0.007$), and SBP ($\beta = -0.01$, $p = 0.014$) were independently associated with longitudinal PDSR after adjustment for other variables (Table 4). When myocardial perfusion parameters upslope and MaxSI were included in multivariable analyses, upslope ($\beta = 0.10$, $p = 0.016$), MaxSI ($\beta = -0.02$, $p = 0.006$), and LDL ($\beta = -0.11$, $p = 0.013$) were independently associated with longitudinal PDSR after adjustment for other variables (Table 4).

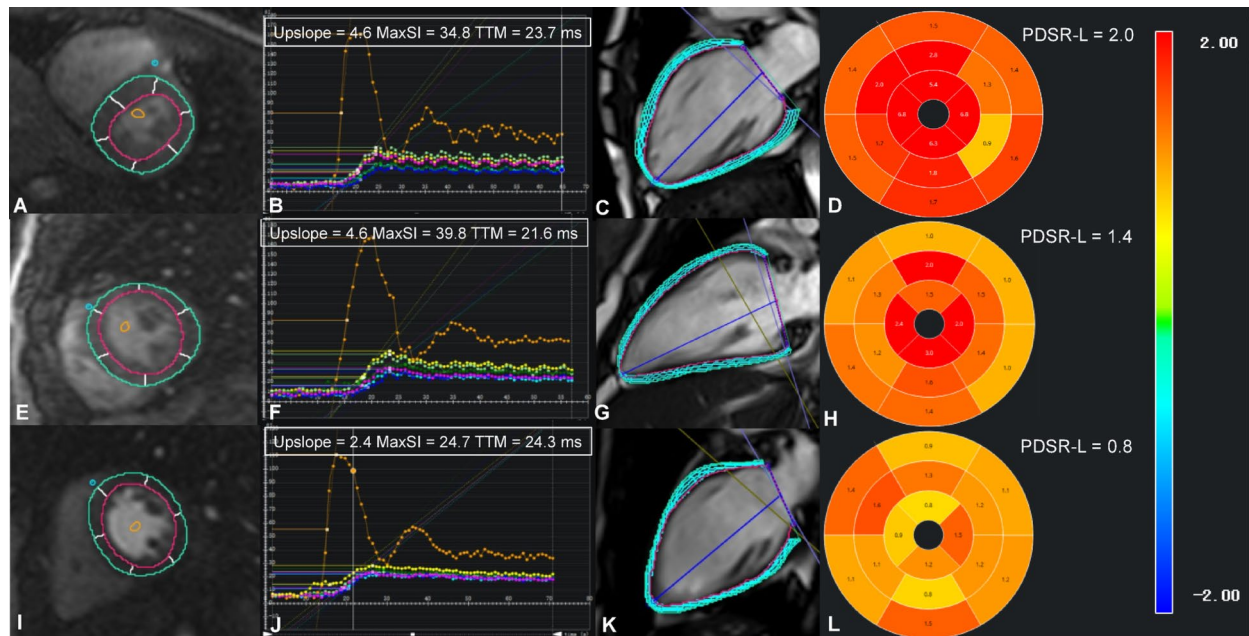


Fig. 3 Representative cases showed myocardial perfusion function and longitudinal peak diastolic strain rate (PDSR-L) in a control (top row), a patient with HbA1c < 7.0% (middle row), and a patient with HbA1c ≥ 7.0% (bottom row). First-pass myocardial perfusion MR images (**A**, **E**, and **I**) and signal intensity-time curves (**B**, **F**, and **J**) were obtained from the left mid-ventricular slices. PDSR-L was analyzed using Bull's-eye plots (**D**, **H**, and **L**) derived from long-axis cine images (**C**, **G**, and **K**). Max SI, maximum signal intensity; TTM, time to maximum signal intensity

Table 3 Univariable and multivariable regression analyses of upslope

Variables	Univariable		Multivariable		
	β (95% CI)	<i>p</i>	β (95% CI)	<i>t</i>	<i>p</i>
Age	-0.20 (-0.29 to -0.12)	< 0.001			
Female	0.06 (-0.59 to 0.71)	0.855 Δ			
BMI	-0.12 (-0.20 to -0.03)	0.008	-0.11 (-0.17 to -0.04)	-3.00	0.005
BSA	-0.03 (-0.06 to 0.00)	0.057			
SBP	-1.93 (-2.94 to -0.92)	< 0.001			
DBP	-0.03 (-0.06 to -0.01)	0.020			
Waist-to-hip ratio	-0.36 (-6.84 to 6.12)	0.915			
Age at diagnosis	-0.06 (-0.15 to 0.03)	0.174			
Duration (years)	-0.03 (-0.13 to 0.07)	0.537 Δ			
HbA1c	-1.87 (-2.90 to -0.84)	< 0.001	-2.53 (-3.53 to -1.54)	-5.00	< 0.001
FBG	-0.06 (-0.14 to 0.02)	0.180			
TC	0.14 (-0.21 to 0.48)	0.444			
TG	-0.54 (-1.41 to 0.34)	0.237			
HDL	0.95 (0.10 to 1.79)	0.033			
LDL	0.03 (-0.36 to 0.42)	0.867 Δ	0.40 (0.08 to 0.73)	2.42	0.021
ApoA1	0.93 (-0.45 to 2.32)	0.195			
Urea nitrogen	0.06 (-0.22 to 0.34)	0.696			
Creatinine	-0.02 (-0.05 to 0.01)	0.160			
Uric acid	-0.01 (-0.99 to -0.01)	0.015			
Cystatin C	-1.85 (-4.84 to 1.14)	0.233			

Variables with $p < 0.1$ and Δ variables based on clinical backgrounds and the absence of collinearity were included in the multivariable analysis. CI confidential interval

Abbreviations are the same as in Table 1

Table 4 Univariable and multivariable regression analyses of longitudinal PDSR

Variables	Univariable		Multivariable ^a			Multivariable ^b		
	β (95% CI)	<i>p</i>	β (95% CI)	<i>t</i>	<i>p</i>	β (95% CI)	<i>t</i>	<i>p</i>
Age	−0.03 (−0.05 to −0.01)	0.005						
Female	−0.01 (−0.14 to 0.11)	0.829 Δ						
BMI	0.00 (−0.02 to 0.02)	0.912 Δ	0.02 (0.01 to 0.03)	2.22	0.030			
BSA	−0.12 (−0.33 to 0.08)	0.250						
SBP	−0.01 (−0.99 to −0.01)	0.035	−0.01 (−0.99 to −0.01)	−2.53	0.014			
DBP	−0.00 (−0.01 to 0.00)	0.146						
Waist-to-hip ratio	0.38 (−0.20 to 0.95)	0.203						
Age at diagnosis	−0.02 (−0.03 to −0.01)	0.005 \square						
Duration (years)	0.01 (−0.01 to 0.02)	0.196 Δ						
HbA1c	−0.31 (−0.45 to −0.16)	<0.001	−0.02 (−0.04 to −0.01)	−2.80	0.007			
FBG	−0.01 (−0.02 to 0.01)	0.354						
TC	−0.03 (−0.08 to 0.01)	0.136						
TG	−0.04 (−0.08 to −0.01)	0.022						
HDL	0.02 (−0.09 to 0.12)	0.772						
LDL	−0.02 (−0.07 to 0.03)	0.369 Δ				−0.11 (−0.19 to −0.03)	−2.67	0.013
ApoA1	0.03 (−0.15 to 0.20)	0.766						
Urea Nitrogen	0.01 (−0.03 to 0.04)	0.754						
Creatinine	−0.00 (−0.01 to 0.00)	0.254						
Uric Acid	0.00 (−0.00 to 0.00)	0.336						
Cystatin C	0.09 (−0.27 to 0.45)	0.622						
Upslope	0.12 (0.05 to 0.19)	<0.001				0.10 (0.02 to 0.18)	2.59	0.016
MaxSI	0.01 (−0.00 to 0.02)	0.167 Δ				−0.02 (−0.03 to −0.01)	−3.03	0.006

Δ Candidate variables for multivariable models were selected based on clinical backgrounds and the absence of collinearity

\square The variable “age at diagnosis” was excluded from multivariable analysis because of collinearity

^aVariables with $p < 0.1$ and Δ based on clinical backgrounds and the absence of collinearity were included in the multivariable analysis

^bPerfusion parameters were added as covariates in the multivariable analysis

PDSR peak diastolic strain rate; Max SI maximal signal intensity, CI confidential interval. Other abbreviations are the same as in Table 1

Table 5 Intra-observer and interobserver reproducibility of CMR parameters

	Intraobserver		Interobserver	
	ICC	95% CI	ICC	95% CI
Myocardial strain				
Radial peak strain	0.937	0.879–0.968	0.936	0.878–0.960
Circumferential peak strain	0.873	0.769–0.932	0.925	0.861–0.960
Longitudinal peak strain	0.895	0.809–0.944	0.917	0.869–0.956
Radial PSSR	0.923	0.850–0.962	0.942	0.884–0.917
Circumferential PSSR	0.895	0.809–0.944	0.874	0.757–0.935
Longitudinal PSSR	0.926	0.832–0.964	0.950	0.866–0.978
Radial PDSR	0.936	0.880–0.967	0.945	0.897–0.971
Circumferential PDSR	0.900	0.817–0.947	0.881	0.766–0.939
Longitudinal PDSR	0.909	0.839–0.952	0.871	0.769–0.930
Myocardial perfusion function				
Upslope	0.982	0.9966–0.990	0.994	0.989–0.997
TTM	0.998	0.994–0.998	0.993	0.887–0.996
MaxSI	0.963	0.931–0.980	0.968	0.941–0.983

ICC intraclass correlation coefficient; other abbreviations same as in Table 2

Inter- and intra-observer variability of CMR-derived parameters

The intra-observer and inter-observer correlation coefficients of the measurement of LV global peak strain,

PDSR, and PSSR in three directions (radial, circumferential, and longitudinal), upslope, TTM, and maxSI were considered good (Table 5).

Discussion

In this study, we included pediatric T1DM patients without other diabetes-related complications to investigate the effect of glycemic levels on the myocardium. We found that (1) pediatric T1DM with HbA1c $\geq 7.0\%$ showed worse myocardial microvascular dysfunction and subclinical diastolic dysfunction. (2) Hyperdynamic systolic function but decreased diastolic function was observed in T1DM with poor control. (3) HbA1c, BMI, and LDL were independently associated with microvascular dysfunction after adjusting for other variables; (4) Myocardial microcirculation dysfunction and LDL were independently associated with reduced LV longitudinal PDSR.

Although the progress of diabetic cardiomyopathy can develop independently of macrovascular complications of the disease, structural and functional changes at the level of the coronary vasculature are common comorbidities in diabetic patients, which can further exacerbate diabetic cardiomyopathy. Currently, most studies have

focused on myocardial perfusion in patients with type 2 diabetes mellitus, while research on myocardial perfusion in T1DM is relatively limited and yields conflicting results [13–15]. Shivu et al. [15] found the average myocardial perfusion reserve index in young asymptomatic subjects with T1DM was significantly lower than that of healthy controls utilizing magnetic resonance spectroscopy and stress magnetic resonance imaging. Our study further confirms that myocardial perfusion dysfunction can be observed at an earlier stage in T1DM patients. Furthermore, higher HbA1c level was associated with worse microvascular dysfunction. Persistent hyperglycemia is associated with endothelial dysfunction [16]. Autopsy studies of ventricular myocardial samples have confirmed the presence of microvascular abnormalities in diabetic patients, including capillary basement membrane thickening, arteriolar intimal thickening, and increased perivascular fibrosis [17, 18]. These microvascular changes are believed to be driven by hyperglycemia, dyslipidemia, and neurohormonal system activation. In the present study, T1DM patients with microcirculatory impairment exhibited poorer control of blood lipids and glucose, further supporting the proposed mechanisms underlying microvascular pathology [16].

Chronic hyperglycemia exacerbates pathological molecular processes such as non-enzymatic glycation, the formation of advanced glycation end products, and oxidative stress. These processes trigger myocardial inflammation, leading to fibrosis, cardiac remodeling, disruption of calcium homeostasis, endothelial dysfunction, and ultimately a decline in myocardial function [19, 20]. Our study revealed impaired longitudinal diastolic myocardial function in the patient groups. Impaired myocardial perfusion was an independent risk factor of longitudinal PDSR. Longitudinal cardiac function of LV depends on the integrity of the subendocardial myocardial fibers, which are more susceptible to microcirculatory damage. LV diastolic dysfunction was potentially driven by microvascular impairment. Furthermore, persistent hyperglycemia is closely linked to endothelial dysfunction, which increases the risk of microvascular permeability, impairs microvascular blood flow, and may lead to tissue ischemia and heart failure [21–23].

Interestingly, our study demonstrated increased longitudinal myocardial contraction accompanied by impaired diastolic function in pediatric T1DM. This observation suggests that diastolic dysfunction may precede systolic impairment in diabetes-related heart disease [24]. The paradoxical hyperdynamic systolic contraction and impaired diastolic function are consistent with previous echocardiographic findings. In the prospective blinded speckle tracking stress echocardiography study, Hensel et al. [25] reported similar results in a cohort of pediatric T1DM with comparable age (mean age 11.5 ± 3.1 years)

and disease duration (mean duration 4.3 ± 3.5 years). Their findings showed that patients with poor glycemic control exhibited increased resting circumferential and longitudinal peak strain despite evidence of reduced diastolic function, as indicated by a decreased E/A ratio. It has also been reported that increased left ventricular torsion in young patients with type 1 diabetes is associated with impaired myocardial perfusion and early diastolic filling abnormalities [15, 26, 27]. This hyperdynamic myocardial contraction in the early stages of diabetes may represent a transient compensatory mechanism in the progression of non-ischemic cardiomyopathy, indicating the onset of the asymptomatic subclinical phase of heart failure [25]. Animal model studies suggest that this phenomenon may be linked to altered myocardial substrate utilization and reduced cardiac efficiency, further deteriorating LV remodeling and systolic function [29, 30].

Existing evidence indicates that patients with diabetic microvascular diseases are prone to have worse clinical adverse outcomes [31]. The screening strategy for T1DM population should include myocardial microvascular disease and not only neuropathy, retinopathy, and nephropathy. These findings highly underscore the critical need for optimizing glycemic control and exploring potential therapeutic strategies to address microvascular dysfunction. Furthermore, CMR offers a noninvasive quantitative method to perform risk stratification in diabetics.

Limitations

The current study has several limitations. First, only CMR perfusion at rest was performed due to the restrictions on medication and the potential risks associated with cardiac stress tests for children. However, the value of rest myocardial perfusion compared to stress perfusion has been validated in a variety of studies with T2DM [13, 32]. Our study has also shown that microvascular function was reduced in T1DM subgroups compared to controls and deteriorated along with elevated HbA1c. The clinical significance of resting myocardial perfusion assessment in T1DM population warrants further attention and validation.

Second, although HbA1c is the most widely used clinical indicator of glycemic control, it may not fully capture glycemic variability or cumulative hyperglycemic exposure. The relationship between cumulative hyperglycemic burden during follow-up and cardiovascular risk requires further investigation.

Third, our single-center design resulted in a modest sample size, though our cohort's glycemic control distribution (75% above target HbA1c) reflects real-world epidemiologic patterns in China [33]. Multicenter prospective studies with larger samples are needed to confirm these findings.

Finally, as all scans were performed at 3.0 T, the potential influence of magnetic field strength on perfusion and strain measurements remains unexplored [34, 35]. Systematic comparisons between 1.5 T and 3.0 T systems in diabetic populations would help establish measurement consistency across platforms.

Conclusions

Pediatric T1DM with higher levels of HbA1c exhibited worse myocardial microvascular function and subclinical diastolic function. HbA1c was independently associated with microvascular dysfunction. Microvascular impairment was an independent risk factor related to reduced subclinical diastolic function.

Abbreviations

T1DM	Type 1 diabetes mellitus
CMR	Cardiac magnetic resonance
HbA1c	Hemoglobin A1c
BSA	Body surface area
BMI	Body mass index
SBP	Systolic blood pressure
DBP	Diastolic blood pressure
FBG	Fast blood glycemia
TC	Total cholesterol
TG	Triglycerides
HDL	High-density lipoprotein
LDL	Low-density lipoprotein
LV	Left ventricular
LVEDVi	Indexed left ventricular end-diastolic volume
LVESVi	Indexed left ventricular end-systolic volume
LVEF	Left ventricular ejection fraction
LVRI	Left ventricular remodeling index
LVMi	Indexed LV mass
PSSR	Global peak systolic strain rate
PDSR	Global peak diastolic strain rate
TTM	Time to maximal signal intensity
Max SI	Maximal signal intensity

Acknowledgements

Not applicable.

Author contributions

Lu Zhang, Conceptualization, Methodology, Formal analysis, Writing-Original draft preparation, Visualization. Shan Huang: Conceptualization, Methodology, Writing-Original draft preparation, Draft revising. Yingkun Guo, Supervision, Project administration, Funding acquisition. Jin Wu, Resources, Conceptualization, Writing-Review & Editing. Pengfei Ye, Resources, Conceptualization. Xueming Li & Ran Sun, Conceptualization, Writing-Review & Editing. Zhi Yang, Resources, Conceptualization. Huayan Xu, Writing-Review & Editing. Rong Xu, Funding acquisition, Writing-Review & Editing. Meng Zhang, Resources, Conceptualization. Chuanjie Yuan, Resources. Ying Liu, Resources.

Funding

This work was supported by the National Natural Science Foundation of China (82120108015, 82271981, 82402251, 82304078, 82302168, and 82482052), Sichuan Science and Technology Program (2023NSFSC1715, 25QNJJ1397, 2024YFFK0259, and 2023ZYD0120), China Postdoctoral Science Foundation (2023M732453), Postdoctoral Fellowship Program of CPS Funder Grant (GZC20231830), and Sichuan University Interdisciplinary Innovation Fund.

Availability of data and materials

No datasets were generated or analysed during the current study.

Declarations

Ethics approval and consent to participate

This study was approved by the Biomedical Research Ethics Committee of our hospital (K2019053) and conducted in accordance with the Declaration of Helsinki. Written informed consent was obtained from all the participants' legal guardian prior to inclusion in the study.

Consent for publication

Not applicable.

Competing interests

The authors declare no competing interests.

Author details

¹Key Laboratory of Birth Defects and Related Diseases of Women and Children (Sichuan University), Ministry of Education, West China Second University Hospital, Sichuan University, Chengdu 614001, Sichuan, China

²Department of Radiology, West China Second University Hospital, Sichuan University, Chengdu 614001, Sichuan, China

³Department of Radiology, West China Hospital, Sichuan University, Chengdu 614001, Sichuan, China

⁴Department of Radiology, Chengdu Fifth People's Hospital, Chengdu 611130, Sichuan, China

⁵Department of Pediatrics, West China Second University Hospital, Sichuan University, Chengdu 614001, Sichuan, China

Received: 22 February 2025 / Accepted: 25 April 2025

Published online: 16 May 2025

References

1. NCD Risk Factor Collaboration (NCD-RisC). Worldwide trends in diabetes prevalence and treatment from 1990 to 2022: a pooled analysis of 1108 population-representative studies with 141 million participants. *Lancet*. 2024;404(10467):2077–2093.
2. Marx N, Federici M, Schütt K, et al. 2023 ESC Guidelines for the management of cardiovascular disease in patients with diabetes: Developed by the task force on the management of cardiovascular disease in patients with diabetes of the European Society of Cardiology (ESC). *Eur Heart J*. 2023;44(39):4043–140.
3. Dabelea D, Stafford JM, Mayer-Davis EJ, et al. Association of type 1 diabetes vs type 2 diabetes diagnosed during childhood and adolescence with complications during teenage years and young adulthood. *JAMA*. 2017;317(8):825–35.
4. Rawshani A, Sattar N, Franzén S, et al. Excess mortality and cardiovascular disease in young adults with type 1 diabetes in relation to age at onset: a nationwide, register-based cohort study. *Lancet*. 2018;392(10146):477–86.
5. Manrique-Acevedo C, Hirsch IB, Eckel RH. Prevention of cardiovascular disease in type 1 diabetes. *N Engl J Med*. 2024;390(13):1207–17.
6. Bjornstad P, Donaghue KC, Maahs DM. Macrovascular disease and risk factors in youth with type 1 diabetes: time to be more attentive to treatment? *Lancet Diabetes Endocrinol*. 2018;6(10):809–820.
7. Lind M, Bounias I, Olsson M, Gudbjörnsdóttir S, Svensson AM, Rosengren A. Glycaemic control and incidence of heart failure in 20,985 patients with type 1 diabetes: an observational study. *Lancet*. 2011;378(9786):140–6.
8. Diabetes Control and Complications Trial (DCCT)/Epidemiology of Diabetes Interventions and Complications (EDIC) Study Research Group. Intensive Diabetes Treatment and Cardiovascular Outcomes in Type 1 Diabetes: The DCCT/EDIC Study 30-Year Follow-up. *Diabetes Care*. 2016;39(5):686–693.
9. Faul F, Erdfelder E, Lang AG, Buchner A. G*Power 3: a flexible statistical power analysis program for the social, behavioral, and biomedical sciences. *Behav Res Methods*. 2007;39(2):175–91.
10. American Diabetes Association Professional Practice Committee. 14. Children and Adolescents: Standards of Care in Diabetes-2024. *Diabetes Care*. 2024;47(Suppl 1):S258–S281.
11. Subspecialty Group of Endocrinologic, Hereditary and Metabolic Diseases, the Society of Pediatrics, Chinese Medical Association, Editorial Board, Chinese Journal of Pediatrics. [Expert consensus on the standardized diagnosis and management of type 1 diabetes mellitus in Chinese children (2020)]. *Zhonghua Er Ke Za Zhi*. 2020;58(6):447–454.

12. Koo TK, Li MY. A guideline of selecting and reporting intraclass correlation coefficients for reliability research. *J Chiropr Med*. 2016;15(2):155–63.
13. Wang J, Yang ZG, Guo YK, et al. Incremental effect of coronary obstruction on myocardial microvascular dysfunction in type 2 diabetes mellitus patients evaluated by first-pass perfusion CMR study. *Cardiovasc Diabetol*. 2023;22(1):154.
14. Byrne C, Jensen T, Hjortkjaer HØ, et al. Myocardial perfusion at rest in patients with Diabetes Mellitus Type 1 compared with healthy controls assessed with Multi Detector Computed Tomography. *Diabetes Res Clin Pract*. 2015;107(1):15–22.
15. Shivu GN, Abozguia K, Phan TT, et al. Increased left ventricular torsion in uncomplicated type 1 diabetic patients: the role of coronary microvascular function. *Diabetes Care*. 2009;32(9):1710–2.
16. Farhangkhoei H, Khan ZA, Kaur H, Xin X, Chen S, Chakrabarti S. Vascular endothelial dysfunction in diabetic cardiomyopathy: pathogenesis and potential treatment targets. *Pharmacol Ther*. 2006;111(2):384–99.
17. Factor SM, Okun EM, Minase T. Capillary microaneurysms in the human diabetic heart. *N Engl J Med*. 1980;302(7):384–8.
18. Kawaguchi M, Techigawara M, Ishihata T, et al. A comparison of ultrastructural changes on endomyocardial biopsy specimens obtained from patients with diabetes mellitus with and without hypertension. *Heart Vessels*. 1997;12(6):267–74.
19. Huynh K, Bernardo BC, McMullen JR, Ritchie RH. Diabetic cardiomyopathy: mechanisms and new treatment strategies targeting antioxidant signaling pathways. *Pharmacol Ther*. 2014;142(3):375–415.
20. Marwick TH, Ritchie R, Shaw JE, Kaye D. Implications of underlying mechanisms for the recognition and management of diabetic cardiomyopathy. *J Am Coll Cardiol*. 2018;71(3):339–51.
21. Di Carli MF, Janisse J, Grunberger G, Ager J. Role of chronic hyperglycemia in the pathogenesis of coronary microvascular dysfunction in diabetes. *J Am Coll Cardiol*. 2003;41(8):1387–93.
22. Camici PG, Tschöpe C, Di Carli MF, Rimoldi O, Van Linthout S. Coronary microvascular dysfunction in hypertrophy and heart failure. *Cardiovasc Res*. 2020;116(4):806–16.
23. Oltman CL, Richou LL, Davidson EP, Coppey LJ, Lund DD, Yorek MA. Progression of coronary and mesenteric vascular dysfunction in Zucker obese and Zucker diabetic fatty rats. *Am J Physiol Heart Circ Physiol*. 2006;291(4):H1780–1787.
24. Ho KL, Karwi QG, Connolly D, et al. Metabolic, structural and biochemical changes in diabetes and the development of heart failure. *Diabetologia*. 2022;65(3):411–23.
25. Hensel KO, Grimmer F, Roskopf M, Jenke AC, Wirth S, Heusch A. Subclinical alterations of cardiac mechanics present early in the course of pediatric type 1 diabetes mellitus: a prospective blinded speckle tracking stress echocardiography study. *J Diabetes Res*. 2016;2016:2583747.
26. Shivu GN, Abozguia K, Phan TT, Narendran P, Stevens M, Frenneaux M. Left ventricular filling patterns and its relation to left ventricular untwist in patients with type 1 diabetes and normal ejection fraction. *Int J Cardiol*. 2013;167(1):174–9.
27. Piya MK, Shivu GN, Tahrani A, et al. Abnormal left ventricular torsion and cardiac autonomic dysfunction in subjects with type 1 diabetes mellitus. *Metabolism*. 2011;60(8):1115–21.
28. Hensel KO, Grimmer F, Roskopf M, Jenke AC, Wirth S, Heusch A. Subclinical alterations of cardiac mechanics present early in the course of pediatric type 1 diabetes mellitus: a prospective blinded speckle tracking stress echocardiography study. *J Diabetes Res*. 2016;2016:2583747.
29. Buchanan J, Mazumder PK, Hu P, et al. Reduced cardiac efficiency and altered substrate metabolism precedes the onset of hyperglycemia and contractile dysfunction in two mouse models of insulin resistance and obesity. *Endocrinology*. 2005;146(12):5341–9.
30. Levelt E, Mahmood M, Piechnik SK, et al. Relationship between left ventricular structural and metabolic remodeling in type 2 diabetes. *Diabetes*. 2016;65(1):44–52.
31. Tromp J, Lim SL, Tay WT, et al. Microvascular disease in patients with diabetes with heart failure and reduced ejection versus preserved ejection fraction. *Diabetes Care*. 2019;42(9):1792–1799.
32. Cao L, Liu C, Ou C, et al. Impact of pretransplant T2DM on left ventricular deformation and myocardial perfusion in heart transplanted recipients: a 3.0 T cardiac magnetic resonance study. *Cardiovasc Diabetol*. 2024;23(1):216.
33. Huo L, Deng W, Shaw JE, et al. Factors associated with glycemic control in type 1 diabetes patients in China: A cross-sectional study. *J Diabetes Investig*. 2020;11(6):1575–82.
34. Holtackers RJ, Wildberger JE, Wintersperger BJ, Chiribiri A. Impact of field strength in clinical cardiac magnetic resonance imaging. *Investig Radiol*. 2021;56(11):764–72.
35. Yang W, Xu J, Zhu L, et al. Myocardial strain measurements derived from MR feature-tracking: influence of sex, age, field strength, and vendor. *JACC Cardiovasc Imaging*. 2024;17(4):364–79.

Publisher's Note

Springer Nature remains neutral with regard to jurisdictional claims in published maps and institutional affiliations.